

# Modeling and optimization of biogas production in a batch bioreactor

Tina Kegl<sup>1</sup>, Eloisa Torres-Jimenez<sup>2</sup>

<sup>1</sup> Faculty of Chemistry and Chemical Engineering  
University of Maribor

Smetanova 17, SI-2000 Maribor (Slovenia)

Phone/Fax number: +386 2 2294 454, e-mail: [tina.kegl@um.si](mailto:tina.kegl@um.si)

<sup>2</sup> Departamento de Ingeniería Mecánica y Minera  
Universidad de Jaén

Edificio A3, despacho 013, Campus las Lagunillas, s/n - 23071 – Jaén (Spain)

Phone/Fax number: +34 953 21 28 67, e-mail: [etorres@ujaen.es](mailto:etorres@ujaen.es)

**Abstract.** Ever increasing demands for renewable energy sources are the driving force for the development of waste management technologies such as anaerobic digestion (AD) technology. For AD process understanding and optimization the numerical simulations provide a useful tool. Therefore, in this work, the main attention is focused on the development of an efficient and stable optimization approach. The optimization procedure is coupled with a suitable mechanistically inspired self-developed BioModel. For BioModel calibration, a special procedure was developed which incorporates the used BioModel, a sensitivity analysis, and a gradient-based optimization algorithm. The results of numerical simulation, obtained by the AD of various animal manures in a batch lab-scale bioreactor, confirm the reliability of BioModel and the efficiency of the presented calibration procedure. Furthermore, the results of AD process optimization show that the biogas quantity and quality as well as energy used up for bioreactor heating can be improved essentially when amount of added bacteria, temperature and pH values are optimized properly.

**Key words.** BioModel, model parameters calibration, activity set optimization procedure, gradient-based optimization algorithm, variable process conditions

## 1. Introduction

In recent times, the interest in biogas technology through anaerobic digestion (AD) has gradually increased due to the energy and environmental benefits it offers. AD technology gives opportunities to reduce a large amount of various types of waste, reduce greenhouse gas emissions to the atmosphere, and produce renewable energy [1]. Namely, AD technology enables a substantial reduction of waste entering landfills and reduction of greenhouse gas emissions in the range between 3,290 and 4,360 Mt CO<sub>2,eq</sub>, which is equivalent to 10-13% of the world's current emissions [2]. Furthermore, in 2020 about 66 billion m<sup>3</sup> of biogas was produced by AD process. The produced amount is equivalent to energy content of 1.52 EJ and it is expected to increase up to 14.4 EJ in 2050 [2].

In general, the AD process can be divided into hydrolysis, acidogenesis, acetogenesis, and methanogenesis, in which microorganisms breakdown organic matter in the absence of oxygen to biogas. The quality and quantity of the produced biogas depend mainly on feedstock substrate and process parameters.

In order to improve the AD performance, a lot of effort is put into the understanding of the AD process by experimental and numerical simulation (NS) studies. Since the experimental studies of the AD process are time consuming, various mechanistically inspired mathematical models were developed already, based on ADM1 [3]-[5] or on BioModel [6]-[10]. Unfortunately, these models include a lot of unknown or hard-to-determine parameters, which have to be calibrated. Till today various more or less efficient procedures were developed for parameters calibration, for example, sensitivity-based hierarchical and sequential single-parameter optimization [11] and active set optimization (ASO) procedure [9]. Proper determination of model parameters is of highest importance for efficient prediction of the AD performance. Furthermore, it is known that only a reliable mathematical model can be incorporated into an optimization problem to improve the AD process. For AD process optimization, various stochastic and deterministic optimization algorithms can be used. However, a direct gradient-based optimization, which may prove to deliver excellent and fast results on certain types of problems, is rarely engaged for the AD process optimization. Moreover, the efficiency of the ASO procedure, coupled with a gradient-based algorithm, is still not verified in a batch bioreactor.

To fill this gap, this paper deals with the modelling and optimization of the AD process in a batch-mode lab-scale bioreactor filled with animal manure. Special attention is focused on the determination of BioModel parameters by ASO procedure and on the usefulness of a gradient-based optimization algorithm for BioModel calibration and AD process optimization.

## 2. Materials and methods

At first, experimental data of the observed AD process are given. Then, the gradient-based optimization algorithm and statistical evaluation methodology are presented briefly.

### A. Experimental data

The AD process, utilizing data of various animal manure in a batch-mode lab-scale bioreactors, was observed. Three separate studies of the AD process on separate bioreactors are performed for BioModel calibration and validation. In all studies, the experimental input data are taken from the literature, Table I. The experimental data for AD of cattle manure [8],[12] was used for BioModel calibration (Cal), while the experimental data for BioModel validation was taken from [13] (buffalo manure, Val 1) and [14] (cow manure, Val 2). Fig. 1 shows the measured AD performance used for BioModel calibration and BioModel validation.

Table I. Input data for BioModel calibration and validation

Parameter	Cal	Val 1	Val 2
Initial insoluble substrate concentration, $c_{is}$ (g/L)	30.4	30.4	30.4
Initial soluble substrate concentration, $c_s$ (g/L)	5.4	5.4	5.4
Initial total acetate concentration, $c_{ac}$ (g/L)	4.5	4.5	4.5
Initial total propionate concentration, $c_{pro}$ (g/L)	2.3	2.3	2.3
Initial total butyrate concentration, $c_{bu}$ (g/L)	0.05	0.05	0.05
Initial total ammonia concentration, $c_{am}$ (g/L)	2.0	2.0	2.0
Liquid volume of bioreactor, $V_{liq}$ (L)	1.0	2.0	0.25
Gas volume of bioreactor, $V_g$ (L)	0.1	0.2	0.01
Total pressure in bioreactor, $p_{total}$ (bar)	1.006	1.073	1.073
pH value, pH (/)	8.0	7.4	7.6
Temperature, $T$ (°C)	35.0	38.5	37.0

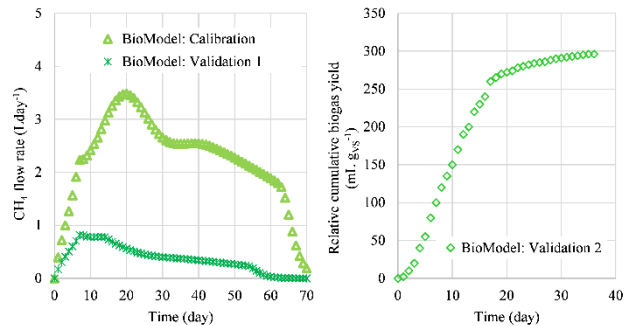


Fig. 1. Measured AD performance, BioModel calibration and validations

In case of BioModel calibration and Val 1, a comparison is made with respect to the  $CH_4$  flow rate. Meanwhile, for Val 2 the relative cumulative biogas yield (mL of the produced biogas per g of volatile solid (VS)) was taken into account. The usage of various lab-scale bioreactors and various input data for BioModel calibration and validation was chosen on purpose. The intent was to demonstrate the wide applicability and robustness of both, the presented ASO procedure and the calibrated BioModel.

### B. Gradient-based optimization algorithm with adaptive approximation scheme

The optimal design problem [14] can be verbally expressed as follows: find such values of design variables  $x_i$ , that while satisfying the constraints  $g_j$ , the value of objective function  $g_0$  is minimized. The used optimization algorithm is based on an approximation method [15], which

sequentially generates approximate, strictly convex, and separable optimization sub-problems and solves them to generate a sequence of converging approximate solutions. The algorithm uses the history of design derivatives of the objective and constraint functions to gradually improve the quality of the approximation; the design derivatives were obtained numerically by using forward differences. This optimal design problem was engaged for BioModel calibration in the proposed ASO procedure as well as for the AD process optimization.

### C. Statistical evaluation methodology

For the evaluation of the proposed BioModel, the measured AD performance is compared by NS using four statistical indicators (SI): (i) mean absolute error,  $\varepsilon_{MAE}$ , (ii) root mean square error,  $\varepsilon_{RMSE}$ , (iii) coefficient of determination,  $R^2$ , and (iv) the relative index of agreement,  $I_{A,rel}$  [10].

## 3. AD process optimization

Since the efficiency of the AD process optimization depends on the reliability of the mathematical model for NS of the AD process, the BioModel was previously calibrated and validated.

### A. BioModel

To simulate the AD process in a batch-mode bioreactor, the BioModel proposed in [8] was used. The main equations of this BioModel are based on continuity equations. In general form, the mass balance equations for concentration of  $i^{\text{th}}$  component in the liquid phase,  $c_{liq,i}$ ,  $i \in N_{liq}$  are given by Eq. (1), while Eq. (2) is used to calculate  $j^{\text{th}}$  biogas component in the gas phase,  $c_{gas,j}$ ,  $j \in N_{gas}$ .

$$\frac{dc_{liq,i}}{dt} = \rho_{bc,i} - \rho_{l-g,i}, \quad i \in N_{liq} \quad (1)$$

$$\frac{dc_{gas,j}}{dt} = \frac{V_{liq}}{V_{gas}} \rho_{l-g,j} - \frac{R T V_{liq}}{(p_{total} - p_w) V_{gas}} \sum_{j \in N_{gas}} \frac{1}{M_j} \rho_{l-g,j} c_{gas,j}, \quad j \in N_{gas} \quad (2)$$

where  $\rho_{bc,i}$  (g/L day<sup>-1</sup>) and  $\rho_{l-g,i}$  (g/L day<sup>-1</sup>) denote the kinetic rates of biochemical and liquid to gas mass transfer processes for  $i^{\text{th}}$  component, respectively. The symbols  $V_{liq}$  (L) and  $V_{gas}$  (L) represent the liquid and gas volumes of the bioreactor,  $p_{total}$  (atm) and  $p_w$  (atm) are total pressure in bioreactor and saturated vapor pressure,  $R$  (atm L mol<sup>-1</sup> K<sup>-1</sup>) is the gas constant,  $T$  (K) is the temperature,  $M_j$  (g mol<sup>-1</sup>) and  $c_{gas,j}$  (g/L) are the molar mass and concentration of  $j^{\text{th}}$  gas component.

The BioModel includes pH- and temperature-dependent parameters, involved into biochemical and physicochemical reactions. Furthermore, in all microbial steps, a non-competitive type of inhibition is used.

The unknown or hard-to-determine parameters in this BioModel are:

- 4 hydrolysis parameters, related to: hydrolysis efficiency  $y_c$ , hydrolysis stoichiometric constants  $n_{hyd}$  and  $m_{hyd}$ , and hydrolysis rate constant  $k_{hyd}$
- 4 inhibition parameters, related to: volatile fatty acids (VFA) inhibition of hydrolysis step  $K_{I,VFA}$ , acetate inhibition of the acetogenic step by propionate  $K_{I,pro}$  and by butyrate  $K_{I,bu}$ , and ammonia inhibition of the methanogenic step  $K_{I,am}$

- 4 Monod saturation constants, related to: Monod saturation constant of soluble substrate  $K_{M,s}$ , propionate  $K_{M,pro}$ , butyrate  $K_{M,bu}$ , and ammonia  $K_{M,am}$
- 32 bacteria factors, related to: maximum specific growth rate at optimal temperature of each type of bacteria,  $\mu_{i,max,T_{opt}}$ , decay coefficients of each bacteria type,  $b_{dec,i}$ , lower and upper pH drop-off value,  $pK_i^{lo}$ ,  $pK_i^{up}$ , temperature coefficient for each bacteria type,  $\alpha_i$ , optimal and maximal temperature for growth of each bacteria type,  $T_{opt,i}$ ,  $T_{max,i}$ , and the initial concentration of each bacteria type in the substrate,  $X_i, i \in I_{bac} = \{A, AP, AB, M\}$
- 4 liquid-gas mass transfer coefficients, related to:  $CO_2$  liquid-gas mass transfer coefficients  $(K_L a)_{CO_2,a}$ ,  $(K_L a)_{CO_2,b}$  and  $CH_4$  liquid-gas mass transfer coefficients  $(K_L a)_{CH_4,a}$ ,  $(K_L a)_{CH_4,b}$ .

These 48 parameters of BioModel were calibrated by ASO procedure with respect to the experimental data.

### B. Sensitivity analysis

At first, a set  $S_x$  of random AD model designs  $x_j, j = 1, \dots, N_S$  (each design  $x_j$  is a complete set of design parameters) is generated. Then, the derivatives of the objective function,  $\frac{\partial g_0}{\partial x_i}$ , for each design  $x_j$  from the set  $S_x$ , are calculated. The objective function  $g_0$  is defined by Eq. (3).

$$g_0 = \int_0^{t_{total}} \left( \frac{Q_{CH_4}(t) - Q_{CH_4,exp}(t)}{Q_{CH_4,exp}} \right)^2 dt \quad (3)$$

where  $t_{total}$  is the total time of the observed AD process,  $Q_{CH_4}(t)$ ,  $Q_{CH_4,exp}(t)$ , and  $\bar{Q}_{CH_4,exp}$  represent time dependent simulated and measured  $CH_4$  flow rates and average value of the measured  $CH_4$  flow rate. After the normalization of the obtained sensitivity results, the importance factor,  $f_{IM,i}$  of each design parameter  $x_i$ , is calculated.

### C. BioModel calibration

The solution of this optimal design problem represents the calibrated values of model parameters; these are obtained by minimizing the daily differences between simulated and measured values of  $CH_4$  flow rates during the total time of the observed AD process,  $t_{total}$ , Eq. (3).

The imposed constraints are related to the sum of concentrations of all considered bacteria types, to the allowed interval between simulated and measured values of  $Q_{CH_4}$  during the total duration of the AD process, and to the total volume of the produced  $CH_4$ . In order to prevent that the optimizer would rise the concentrations of bacteria beyond realistic values, a constraint function  $g_1$ , is related to maximal allowed bacteria concentration in the substrate, Eq. (4). For stability reasons, the quantity  $Q_{CH_4}$  is required to be within the interval  $[k_{Q_{CH_4}}^{LO} Q_{CH_4,exp}, k_{Q_{CH_4}}^{UP} Q_{CH_4,exp}]$  for any  $t \in [0, t_{total}]$ ; the factors  $k_{Q_{CH_4}}^{LO} < 1$  and  $k_{Q_{CH_4}}^{UP} > 1$  define the width of the allowed interval for the  $i^{th}$  performance quantity  $Q_{CH_4,exp}$ . To fulfill this requirement, the lower limit of quantity  $Q_{CH_4}$  is constrained by Eq. (5) while Eq. (6) constrains the upper limit of  $Q_{CH_4}$ . Note that the inverse tangent function in these constraints was used as a differentiable substitute for the conventional step function; this is necessary to preserve the differentiability of the involved functions, which is a requirement if a gradient-based optimizer will be engaged. By Eq. (7) the maximal

difference between measured and calculated total volume of the produced  $CH_4$  is constrained.

$$g_1 = \frac{\sum_i x_i - x_{bac}^{max}}{x_{bac}^{max}}, i \in I_{bac} \quad (4)$$

$$g_2 = \frac{\int_0^{t_{total}} \left( 0.5 + \tan^{-1} \left( \frac{10 \tau^{LO}}{Q_{CH_4,exp}} \right) \tau^{LO} \right) dt}{t_{total} \bar{Q}_{CH_4,exp}} \quad (5)$$

$$g_3 = \frac{\int_0^{t_{total}} \left( 0.5 + \tan^{-1} \left( \frac{10 \tau^{UP}}{Q_{CH_4,exp}} \right) \tau^{UP} \right) dt}{t_{total} \bar{Q}_{CH_4,exp}} \quad (6)$$

$$g_4 = [V_{CH_4,exp} - V_{CH_4}] - \Delta V_{CH_4,max} \quad (7)$$

where  $x_{bac}^{max}$  ( $gL^{-1}$ ) represents the maximal allowed bacteria concentration,  $Q_{CH_4,exp}$  ( $Lday^{-1}$ ) and  $\bar{Q}_{CH_4}$  ( $Lday^{-1}$ ) are measured and predicted  $CH_4$  flow rates,  $\bar{Q}_{CH_4,exp}$  ( $Lday^{-1}$ ) denotes the average value of the measured  $CH_4$  flow rates,  $\tau^{LO} = k_{Q_{CH_4}}^{LO} Q_{CH_4,exp} - Q_{CH_4}$ ,  $\tau^{UP} = Q_{CH_4} - k_{Q_{CH_4}}^{UP} Q_{CH_4,exp}$ ,  $k_{Q_{CH_4}}^{LO} (/)$  and  $k_{Q_{CH_4}}^{UP} (/)$  are factors which define lower and upper limits of interval,  $V_{CH_4,exp}$  (L) and  $V_{CH_4}$  (L) are measured and calculated total volume of the produced  $CH_4$ . All constraints, Eqs. (4)-(7), are imposed in the standard form  $g_i \leq 0, i = 1 \dots 4$ . Our BioModel represents the response equation in the optimal design problem. All of the 48 BioModel parameters are chosen as design variables.

### D. ASO procedure

The ASO procedure [9] incorporates the used BioModel, a sensitivity analysis and a gradient-based optimization algorithm in order to calibrate the BioModel parameters. The initial values of the all design variables are the recommended values from the available literature. The calibration of all BioModel parameters is performed in several cycles. At the beginning of the first cycle, some initial and a relatively high activation threshold value  $f_T$  was chosen to determine a relatively low number of active design parameters. Within each cycle, the active design variables  $x_i^*$  are determined for which it holds  $f_{IM,i} \geq f_T$ ; all other design variables are designated as passive in the current cycle. The values of active design parameters are optimized while keeping the passive ones constant at their recommended values. After that a new cycle with a lower value of  $f_T$  is started until all design variables are active and calibrated by the optimization process.

### E. AD process optimization

The selected design variables in the AD process are related to the biological additive, represented by four bacteria groups ( $X_{i,add}, i \in I_{bac}$ ) and to the AD process conditions, such as temperature and pH value. With respect to the chosen design variables, three modes of the AD process optimization are considered.

**Mode 1.** Temperature and pH value are assumed constant during the AD process.

**Mode 2.** Temperature and pH value are defined by using piecewise linear function; 5 non-uniform segments are used [8].

**Mode 3.** Temperature and pH value are defined by 5<sup>th</sup> order Bezier function; the control points' locations are uniformly distributed along the process time interval [8].

In all modes, the initial concentrations of added 4 bacteria groups were included as design variables. So, in Mode 1 the

values of 6 design variables have to be optimized, while in Modes 2 and 3, we have 18 design variables.

Related to the definition of the objective and constraint functions, two cases were considered.

**Case A.** Objective function is defined as a negative time-integrated biogas volume produced, Eq. (8)

$$g_0 = -\frac{1}{\psi_A} \int_0^{t_{\text{total}}} V_{\text{biogas}}(t) dt \quad (8)$$

where  $\psi_A$  is a normalization constant. The minimization of this objective function, Eq. (8), maximizes the total biogas volume.

Besides the upper and lower limits of the design variables, an additional constraint was related to the allowed maximal initial concentration of all bacteria (present in the influent substrate and added as biological additive), Eq. (9).

$$g_1 = \frac{\sum_{i \in I_{\text{bac}}} (X_i + X_{i,\text{add}}) - X_{\text{max}}}{X_{\text{max}}} \quad (9)$$

**Case B.** The objective function is a sum of two quantities: negative produced biogas and positive heating cost, multiplied by adequate weighting factors, Eq. (10)

$$g_0 = -\frac{\varphi_{B,1}}{\psi_{B,1}} \int_0^{t_{\text{total}}} V_{\text{biogas}}(t) dt + \frac{\varphi_{B,2}}{\psi_{B,2}} \int_0^{t_{\text{total}}} (T - T_{\text{ref}}) dt \quad (10)$$

where  $\varphi_{B,1}$  and  $\varphi_{B,2}$  are weighting factors,  $\psi_{B,1}$  and  $\psi_{B,2}$  are normalization constants,  $T \geq T_{\text{ref}}$  is the enforced design-dependent bioreactor temperature, and  $T_{\text{ref}}$  is a reference temperature, that would be present in the bioreactor without heating.

Besides the upper and lower limitation of the design variables and the allowed maximal concentration of the maximal initial concentration of all bacteria, Eq. (9), the additional constraints are related to the  $\text{CH}_4$  content in the produced biogas by Eqs. (11)-(12).

$$g_2 = \frac{V_{\text{CH}_4}}{V_{\text{biogas}}} - \varphi_{\text{CH}_4,\text{max}} \quad (11)$$

$$g_3 = \varphi_{\text{CH}_4,\text{min}} - \frac{V_{\text{CH}_4}}{V_{\text{biogas}}} \quad (12)$$

where  $\varphi_{\text{CH}_4,\text{max}}$  and  $\varphi_{\text{CH}_4,\text{min}}$  denote maximal and minimal fraction of  $\text{CH}_4$  in the produced biogas.

## 4. AD process optimization

The BioModel, the ASO procedure and the whole optimization procedure were coded in-house in the C# language. The system of ODEs was solved by the Euler method. To improve numerical performance, the computation of design derivatives was parallelized. In this scenario, one full optimization cycle for BioModel calibration (48 design variables being active) took about 3 seconds and for AD process conditions optimization about 1 second on an 8-core i7 CPU desktop computer. The number of optimization cycles, needed to obtain optimum model and process parameters, ranged usually around 200. At first, the results of the AD process modeling are presented, followed by the results of the AD process optimization.

### A. AD process modeling

At first, the results of sensitivity analysis are presented, followed by the results of BioModel calibration and validation.

**Sensitivity analysis.** The most important model parameters are: ammonia inhibition constant,  $K_{i,\text{am}}$ , maximal methanogenic bacteria growth rate at optimal temperature,

$\mu_{M,\text{max},T_{\text{opt}}}$ , hydrolysis stoichiometric constant,  $n_{\text{hyd}}$ , hydrolysis efficiency,  $y_c$ , initial concentration of methanogenic bacteria,  $X_M$ , Monod saturation constant of soluble organic matter,  $K_{M,S}$ , factor of methanogenic bacteria decay  $b_{\text{dec},M}$ , hydrolysis stoichiometric constant,  $m_{\text{hyd}}$ , upper pH drop-off value for methanogenic bacteria,  $pK_M^{\text{up}}$ , and maximal acidogenic bacteria growth rate at optimal temperature,  $\mu_{A,\text{max},T_{\text{opt}}}$ .

**BioModel calibration.** The optimal values of design parameters,  $x_i$ ,  $i = 1 \dots N_x$  are given in Table II.

Table II. Optimal values of design parameters.

$i$	Parameter	Optimal value	$i$	Parameter	Optimal value
1	$X_{\text{Asu}}$ (gL <sup>-1</sup> )	0.29131	25	$K_{i,H_2,S,\text{Ava}}$ (gL <sup>-1</sup> )	0.47697
2	$X_{\text{Aaa}}$ (gL <sup>-1</sup> )	0.29092	26	$K_{i,H_2,S,\text{Mac}}$ (gL <sup>-1</sup> )	0.50035
3	$X_{\text{Agly}}$ (gL <sup>-1</sup> )	0.29108	27	$K_{i,H_2,S,\text{Mhyd}}$ (gL <sup>-1</sup> )	0.46746
4	$X_{\text{Aoa}}$ (gL <sup>-1</sup> )	0.29144	28	$K_{i,H_2,S,\text{Ss}}$ (gL <sup>-1</sup> )	0.48012
5	$X_{\text{Apro}}$ (gL <sup>-1</sup> )	0.30138	29	$K_{i,H_2,S,\text{Spro}}$ (gL <sup>-1</sup> )	0.48043
6	$X_{\text{Abu}}$ (gL <sup>-1</sup> )	0.30078	30	$K_{i,H_2,S,\text{Sac}}$ (gL <sup>-1</sup> )	0.48051
7	$X_{\text{Ava}}$ (gL <sup>-1</sup> )	0.29793	31	$K_{i,H_2,S,\text{Shyd}}$ (gL <sup>-1</sup> )	0.48081
8	$X_{\text{Mac}}$ (gL <sup>-1</sup> )	0.30778	32	$K_{i,\text{NH}_3,\text{Mac}}$ (gL <sup>-1</sup> )	0.22095
9	$X_{\text{Mhyd}}$ (gL <sup>-1</sup> )	0.10299	33	$K_{i,\text{Cu}^{2+},\text{Abu}}$ (gL <sup>-1</sup> )	0.48041
10	$X_{\text{Spro}}$ (gL <sup>-1</sup> )	0.28040	34	$K_{i,\text{Zn}^{2+},\text{Abu}}$ (gL <sup>-1</sup> )	0.48038
11	$X_{\text{Sac}}$ (gL <sup>-1</sup> )	0.29094	35	$K_{i,\text{Cr}^{2+},\text{Abu}}$ (gL <sup>-1</sup> )	0.48008
12	$X_{\text{Ss}}$ (gL <sup>-1</sup> )	0.29112	36	$K_{i,\text{Pb}^{2+},\text{Abu}}$ (gL <sup>-1</sup> )	0.48041
13	$X_{\text{Shyd}}$ (gL <sup>-1</sup> )	0.28475	37	$K_{i,\text{Ni}^{2+},\text{Abu}}$ (gL <sup>-1</sup> )	0.48041
14	$k_{\text{hyd,ch}}$ (day <sup>-1</sup> )	5.44266	38	$K_{i,\text{Cu}^{2+},\text{Mac}}$ (gL <sup>-1</sup> )	0.48044
15	$k_{\text{hyd,pr}}$ (day <sup>-1</sup> )	4.95942	39	$K_{i,\text{Zn}^{2+},\text{Mac}}$ (gL <sup>-1</sup> )	0.48052
16	$k_{\text{hyd,ii}}$ (day <sup>-1</sup> )	5.01598	40	$K_{i,\text{Cr}^{2+},\text{Mac}}$ (gL <sup>-1</sup> )	0.47892
17	$K_{i,\text{VFA}}$ (gL <sup>-1</sup> )	0.22880	41	$K_{i,\text{Pb}^{2+},\text{Mac}}$ (gL <sup>-1</sup> )	0.48042
18	$K_{i,H_2,\text{Agly}}$ (gL <sup>-1</sup> )	0.05280	42	$K_{i,\text{Ni}^{2+},\text{Mac}}$ (gL <sup>-1</sup> )	0.48042
19	$K_{i,H_2,\text{Aoa}}$ (gL <sup>-1</sup> )	0.05280	43	$K_{M,\text{Ni}_0}$ (gL <sup>-1</sup> )	0.00528
20	$K_{i,H_2,\text{Apro}}$ (gL <sup>-1</sup> )	0.05284	44	$K_{M,\text{P}_0}$ (gL <sup>-1</sup> )	0.00527
21	$K_{i,H_2,\text{Abu}}$ (gL <sup>-1</sup> )	0.05280	45	$k_{M,\text{suAsu}}$ (gL <sup>-1</sup> )	0.47809
22	$K_{i,H_2,\text{Ava}}$ (gL <sup>-1</sup> )	0.05279	46	$k_{M,\text{aaAaa}}$ (gL <sup>-1</sup> )	0.47919
23	$K_{i,H_2,S,\text{Apro}}$ (gL <sup>-1</sup> )	0.48386	47	$k_{M,\text{glyAgly}}$ (gL <sup>-1</sup> )	0.47978
24	$K_{i,H_2,S,\text{Abu}}$ (gL <sup>-1</sup> )	0.47729	48	$k_{M,\text{oaAoa}}$ (gL <sup>-1</sup> )	0.47888

By using the proposed ASO procedure, various sets of active design variables are generated with respect to the prescribed threshold,  $f_T$ . By decreasing  $f_T$  from 0.2 to 0.0, the number of active design variables increases gradually from 9 to 48; by including more design variables, the values of the objective function decrease monotonically.

The  $\text{CH}_4$  flow rates, obtained by NS with the initial and various optimal values of design parameters (computed with active Sets from 1 to 5, Set 5 represents the optimal design), are compared to the measured data in Fig. 5. The average values of  $\text{CH}_4$  flow rate, obtained with initial values of design parameters, differs from the averaged measured values approximately by 54.5% (average absolute daily difference divided by average daily measurement). By far the largest improvement of this result (difference lower than 1%) is reached by optimizing the active design variables of Set 1. Further optimization of the Sets 2 to 5 gradually also improves the result but the improvements are becoming progressively small. It is clearly evident that the dynamics of the  $\text{CH}_4$  flow rate obtained with optimal values of all 48 design parameters, presented in Fig. 5 is the closest to the dynamics of the measured  $\text{CH}_4$  flow rate. The average difference is approximately less than 1%; therefore, the calculated  $\text{CH}_4$  flow rates agrees very well with the measured values.

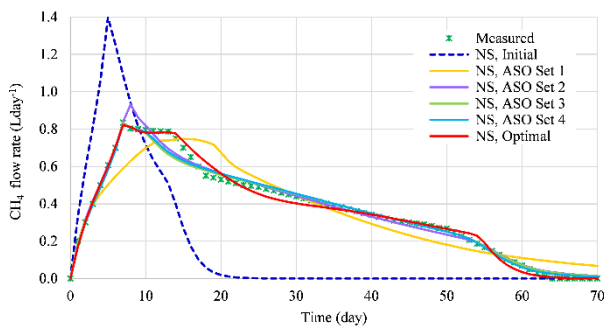


Fig. 5. Time evolution of CH<sub>4</sub> flow rate, model calibration.

SI are given in Table III. It can be seen that by including more design variables, all SI show better agreement between the simulated and experimentally obtained  $Q_{CH_4}$ ; namely, the indicators  $\epsilon_{MAE}$  (Lday<sup>-1</sup>) and  $\epsilon_{RMSE}$  (Lday<sup>-1</sup>) decrease, while the indicators  $R^2$  (/) and  $I_{A,rel}$  (/) increase. According to the presented results, one can say that the optimization of the most important parameters (Set 2) yields relatively good results. For the fine tuning, however, the activation of all design parameters (Set 5, optimal design) may be worth a consideration.

Table III. SI for  $Q_{CH_4}$ , BioModel calibration.

SI	Initial design	Optimal design – ASO procedure				
		Set 1	Set 2	Set 3	Set 4	Optimal
$\epsilon_{MAE}$	0.2875	0.0632	0.0196	0.0176	0.0174	0.0180
$\epsilon_{RMSE}$	0.3411	0.0794	0.0297	0.0289	0.0265	0.0245
$R^2$	0.5218	0.8915	0.9848	0.9879	0.9889	0.9901
$I_{A,rel}$	0.6771	0.9705	0.9961	0.9962	0.9962	0.9974

**BioModel validation.** The validation of the calibrated BioModel was done by using a separate set of measured data [13],[14]. The agreement between the calculated and measured CH<sub>4</sub> flow rates is given in Fig. 6a. The calculated CH<sub>4</sub> flow rates agrees very well with the measured data through the whole interval of the AD process observation. However, the calculated average CH<sub>4</sub> flow rates, differ on measured average values by around 8%. The agreement between calculated and measured relative cumulative biogas yields is given in Fig. 6b. The simulated AD performance agrees very well with the measured data through the whole interval of the AD process observation; differences are less than 10%.

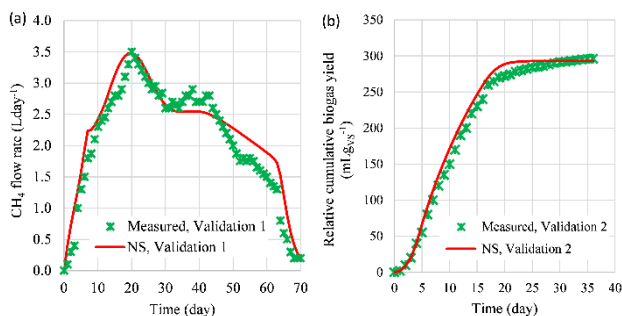


Fig. 6. AD performance using calibrated BioModel: (a) Val 1, (b) Val 2.

All calculated SI as well as good agreement of the AD performance in various bioreactors under various conditions confirm the reliability of the calibrated BioModel. Furthermore, it confirms also the wide applicability of the ASO procedure. Therefore, this BioModel can be incorporated into the AD process optimization procedure.

## B. AD process optimization

The BioModel with calibrated values of model parameters is used for further AD process optimization. The optimized values of design variables are presented in Figs. 7-8. Fig. 7 shows the initial concentration of bacteria (initial design; the concentration of bacteria presents in animal manure) and the concentration of the added bacteria (optimal design). The total initial bacteria concentration (bacteria present in substrate + added bacteria) of all bacteria is limited by the maximal value of  $X_{max} = 2 \text{ gL}^{-1}$ .

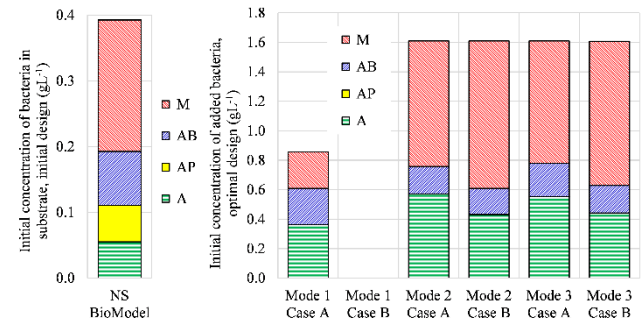


Fig. 7. Bacteria in substrate and added bacteria.

The added amount of the bacteria in optimal designs of Mode 1 is smaller than in other two modes; in Mode 1, Case B there is actually no added bacteria. In optimal designs of Mode 2 and 3, in Case A, over 50% of added bacteria belongs to methanogenic bacteria, around 35% to the acidogenic bacteria, and the rest to the acetogenic bacteria. In Case B, the methanogenic bacteria represent over 60% and acidogenic bacteria around 27%.

Time evolution of pH values and temperature is presented in Fig. 8 for initial and optimal designs. In order to maximize biogas production (Case A) in all modes, optimal conditions are reached at pH value lower than 7.3, Fig. 8. In Case B, Mode 2 and Mode 3, the pH value increases from 7.0 to 7.8 during the AD process; after main biogas production, the pH value approaches to the optimized pH value at Mode 1, where the constant pH value is considered. As it is evident from Fig. 8, in order to maximize biogas production (Case A) in all modes, the optimal values of temperature is around 55 °C. In Case B in Mode 2 and Mode 3, the temperature decreases during the AD process from 55 °C to 25 °C, which is the optimal temperature in Mode 1, Case B.

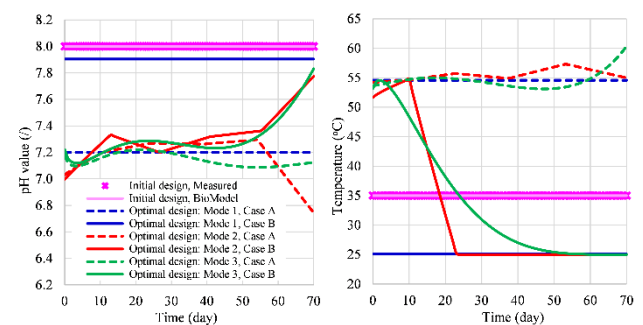


Fig. 8. Time evolution of pH values and temperature.

The AD performance of various optimal designs, compared to those obtained by NS using BioModel and experiment of the initial design, are given in Fig. 9.

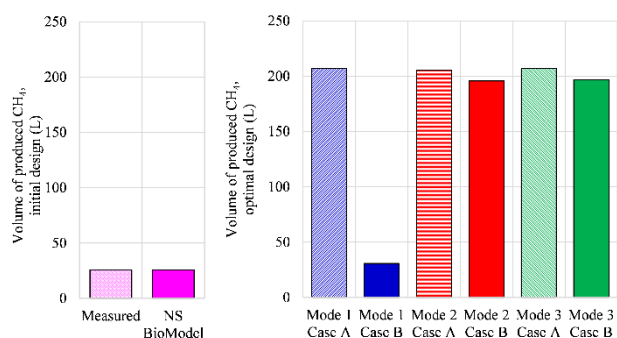


Fig. 9. Time evolution of produced CH<sub>4</sub>.

It can be seen that for all modes, Case A enables higher CH<sub>4</sub> production than Case B. The main reason lies in the higher optimized values of temperature in Case A, which is obtained during optimization without minimization of heating-related cost and without requirements of higher content of CH<sub>4</sub> in the produced biogas. This high temperature, Fig. 8, is the main reason to increase the produced biogas (Case A) and this is in the accordance with the fact, that thermophilic temperature can enable higher biogas production [8],[16]. In Case B, where the heating cost is included into the objective function, the low optimal values of temperature and consequently lower produced biogas are reached, but the content of CH<sub>4</sub> in biogas is higher. Another observation that can be made is that the possibility to adjust the temperature and pH histories can contribute to improve the results. Namely, it is obvious that variable temperature and pH histories enable high CH<sub>4</sub> production at relatively low heating costs. Both, Mode 2 and Mode 3, deliver good results in term of biogas production, but the optimal piecewise linear function exhibits sharp variations with large gradients and might be difficult to enforce in practice. From this point of view, it seems that the best optimal design is obtained using the Bezier time dependent function and by the multiple objectives related to the maximization of the biogas production and minimization of heating-related cost.

## 5. Conclusions

The obtained results of modeling and optimization of the AD process in a batch-mode lab-scale bioreactor confirm the reliability of the used BioModel and the efficiency of the proposed ASO procedure for parameters calibration; all values of the SI are satisfactory. Furthermore, the engaged gradient-based optimization algorithm with adaptive approximation scheme proved to be computationally efficient for BioModel calibration and for AD process optimization. The highest CH<sub>4</sub> production at relatively low heating costs is achieved by variable temperature in pH histories, which follow the Bezier time dependent functions, and by the definition of multi-objective function including the maximization of the biogas production and minimization of heating-related cost.

## Acknowledgements

The authors are grateful for the financial support of the Slovenian Research Agency (core research funding No. P2-0414) and of the University of Jaén (Acción 1a PAIUA 2021-2022). Tina Kegl also highly appreciates the fellowship granted by L'Oréal-UNESCO, Slovenia, under the program "For Women in Science 2022".

## References

- [1] A.A. Issah, T. Kabera, F. Kemausuor, "Biogas optimization processes and effluent quality: A review", *Biomass and Bioenergy* (2020). Vol. 133, 105449.
- [2] B. Aghel, S. Behaein, S. Wongwises, M. Safdari Shadho. "A review of recent progress in biogas upgrading: With emphasis on carbon capture", *Biomass and Bioenergy* (2022). Vol. 160, 106422.
- [3] D.J. Batstone, J. Keller, I. Angelidaki, S.V. Kalyuzhnyi, S.G. Pavlostathis, A. Rozzi, W.T.M. Sanders, H. Siegrist, V.A. Vavilin, *Anaerobic Digestion Model No. 1 (ADM1)*, IWA Publishing, London (2002).
- [4] L. Frunzo, F.G. Feroso, V. Luongo, M.R. Mattei, G. Esposito, "ADM1-based mechanistic model for the role of trace elements in anaerobic digestion processes", *Journal of Environmental Management* (2019). Vol. 241, pp. 587-602.
- [5] H. Sun, Z. Yang, Q. Zhao, M. Kurbonova, R. Zhang, G. Liu, W. Wang, "Modification and extension of anaerobic digestion model No.1 (ADM1) for syngas biomethanation simulation: From lab-scale to pilot-scale", *Chemical Engineering Journal* (2021). Vol. 403, 126177.
- [6] I. Angelidaki, L. Ellegaard, B.K. Ahring, "A mathematical model for dynamic simulation of anaerobic digestion of complex substrates: Focusing on ammonia inhibition", *Biotechnology and Bioengineering* (1993). Vol. 42, pp. 159-166.
- [7] A. Kovalovszki, M. Alvarado-Morales, I.A. Fotidis, I. Angelidaki, "A systematic methodology to extend the applicability of a bioconversion model for the simulation of various co-digestion scenarios", *Bioresource Technology* (2017). Vol. 235, pp. 157-166.
- [8] T. Kegl, A. Kovač Kralj, "Multi-objective optimization of anaerobic digestion process using a gradient-based algorithm", *Energy Conversion and Management* (2020). Vol. 226, 113560.
- [9] T. Kegl, A. Kovač Kralj, "An enhanced anaerobic digestion BioModel calibrated by parameters optimization based on measured biogas plant data", *Fuel* (2022). Vol. 312, 122984.
- [10] T. Kegl, "Consideration of biological and inorganic additives in upgraded anaerobic digestion BioModel", *Bioresource Technology* (2022). Vol. 355, 127252.
- [11] W. Ahmed, J. Rodríguez, "Generalized parameter estimation and calibration for biokinetic models using correlation and single variable optimisations: Application to sulfate reduction modelling in anaerobic digestion", *Water Research* (2017). Vol. 122, pp. 407-418.
- [12] A. Keshtkar, H. Ghaforian, G. Abolhamd, B. Meyssami, "Dynamic simulation of cyclic batch anaerobic digestion of cattle manure", *Bioresource Technology* (2001). Vol. 80, pp. 9-17.
- [13] E.M. Abdelsalam, M. Samer, M.A. Abdel Hadi, H.E. Hassan, Y. Badr, "The effect of buffalo dung treatment with paunch fluid on biogas production", *Misr Journal of Agricultural Engineering* (2015). Vol. 32, pp. 807-826.
- [14] L. Adelard, T.G. Poulsen, V. Rakotoniaina, "Biogas and methane yield in response to co-and separate digestion of biomass wastes", *Waste Management & Research* (2015). Vol. 33, pp. 55-62.
- [15] M. Kegl, B.J. Butinar, B. Kegl, "An efficient gradient-based optimization algorithm for mechanical systems", *Communications in Numerical Methods in Engineering* (2002). Vol. 18, pp. 363-371.
- [16] S.A. Neshat, M. Mohammadi, G.D. Najafpour, P. Lahijani, "Anaerobic co-digestion of animal manures and lignocellulosic residues as a potent approach for sustainable biogas production", *Renewable and Sustainable Energy Reviews* (2017). Vol. 79, pp. 308-322.